



Eidgenössische Technische Hochschule Zürich
Swiss Federal Institute of Technology Zurich



Au NWs/MWCNTs/Au NWs transparent and stretchable current collector for Li-ion batteries

Semester Project I

Luca Mondonico

19-945-641

`lmondonico@student.ethz.ch`

Supervisor: Prof. Markus Niederberger

ETH Zürich

Acknowledgements

I thank...

PROF. DR. MARKUS NIEDERBERGER for having me as part of the multifunctional materials group at ETH Zürich.

TIAN LIU for the precious help and guidance during this research project.

Introduction

As often seen in science fiction films, it is anticipated that futuristic technology will eventually be in the form of portable devices. In recent times, transparent and wearable electronic devices such as smart glasses, electronic maps or flexible screens are gaining tremendous scientific and social attention. However, they still contain a lot of opaque and rigid electronic parts, thus making it hard to truly call them “transparent and wearable” electronics. Therefore, these flexible devices will require electrodes with not only high transparency and electrical conductivity, but also good mechanical compliance. Indeed, during standard operations these devices will undergo different mechanical deformations, ranging from stretching and bending up to twisting and folding. In the last decade, many alternatives to conventional materials have been suggested. For instance, ITO (indium tin oxide) was proposed due to its high transparency and conductivity; however, intrinsic drawbacks of ITO film, such as its brittleness, limited indium resources³, and high fabrication expense due to high-temperature or vacuum processing⁴ limit its use in wearable flexible devices. Carbon nanotubes (CNTs)^{5,6}, graphene^{7,8} and metallic nanowires (NWs)⁹⁻¹¹ have also been introduced. Despite displaying optimal elasticity, flexibility and stretchability, CNTs often suffer from relatively poor electric conductivity (EC), thus low transparency to achieve moderate conductivity. Metallic NWs tend to manifest complementary properties. Metallic NWs, especially Ag NWs ($EC \approx 6.3 \cdot 10^5$ S/cm)¹² and Au NWs ($EC \approx 4.52 \cdot 10^5$ S/cm)¹³ have high conductivity because of the high electron density of the constituting metals, but also flexible and elastic. This said, metallic NWs still managed to be used, for instance as transparent electrodes substitutes in the manufacturing of flexible solar cells. Each of these materials has its own strengths and weaknesses, which are inevitably reflected in the performances of the resultant conductor. One of the main objectives of this Semester Project is to combine two different materials in order to account for each material’s shortcomings with each other’s strength; we attempt to resolve the existing limitations of stretchable electronics by implementing hybrid nanocomposites using a hierarchical transparent structure. The proposed hybrid material is a hierarchical multiscale Au NWs/Multi-walled carbon nanotubes (MWCNTs)/Au NWs nanocomposite percolation network upon a flexible, transparent and hexagonal-structured PDMS membrane, with gold nanowires with relatively smaller dimension ($\varnothing \approx 3$ nm, $L \approx 50-100$ μ m) and MWCNTs with relatively smaller length but larger dimension ($\varnothing \approx 11$ nm, $L \approx 5-20$ μ m). In this research, we prepared a Au NWs/MWCNTs/Au NWs hybrid nanocomposite current collector with the enhanced mechanical compliance and optical

transparency. The final structure is proved to be conductive (average resistance of 40-50 Ω), transparent (T: 80-85%), highly stretchable (up to 100% strain) with consistent mechanical reliability over long repeated bending/stretching cycles (1000 cycles).

Results and discussion

We report in **Figures 1a,1b** and **1c** a simplified 3D scheme of the hierarchical multiscale Au NWs/MWCNTs/Au NWs nanocomposite conductor that was prepared. As suggested by previous research studies¹⁴, the presence of a multilayered structure formed by various materials of different sizes and conductivities may generate and enhance electron transport across different scales^{15,16}. For the hybrid conductor, highly conductive Au NWs percolation networks provide backbone electrodes for a fast electron transport, while the quite resistive but elastic MWCNTs carpet guarantees both stretchability and flexibility. In addition to this, the carbon nanotubes can provide local path for electrons which will be further collected by the electron freeway of the Au NWs backbone mesh. A simplified sketch of the multiscale electron transport in our hierarchical nanocomposite is shown in **Figures 1d** and **1e**.

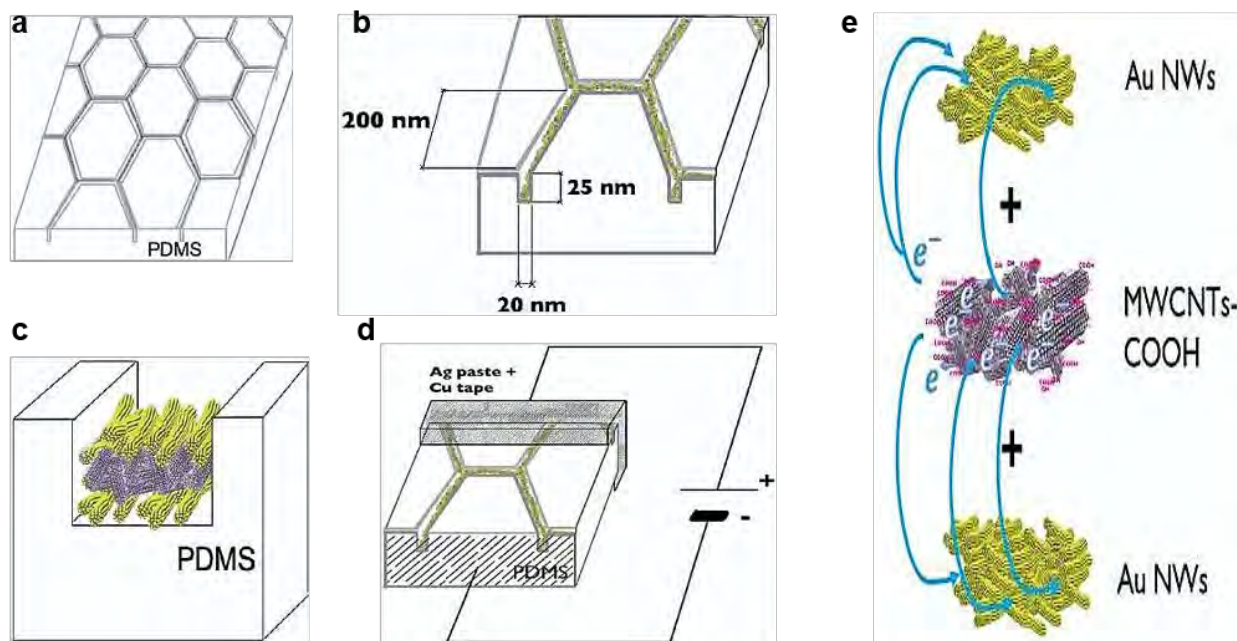


Figure 1. (a) hexagonal grid on the PDMS membrane; (b) size of the channels and characteristic dimensions of the grid; (c) cross-section of a channel on the PDMS substrate; (d) 3D scheme of the hybrid current collector when a certain voltage is applied to two opposite sides; (e) multiscale electron transport in the Au NWs/MWCNTs/Au NWs layered structure.

Transmittance measurements were performed using an integrated-sphere-combined UV/Vis spectrophotometer. Considering only the first layer of Au NWs, different Au NWs volumes were tested: 0.2 mL, 0.6 mL, 1.0 mL and 1.4 mL. All the volumes were spray-coated with nitrogen gas at a pressure of 0.5 bar. **Figure 2e** shows the transmittance in the visible range for the four tested sample: at a reference wavelength of 550 nm, the transmittances of 82.8%, 81.4%, 81.0% and 80.3% were obtained for volumes of 0.2 mL, 0.6 mL, 1.0 mL and 1.4 mL, respectively.

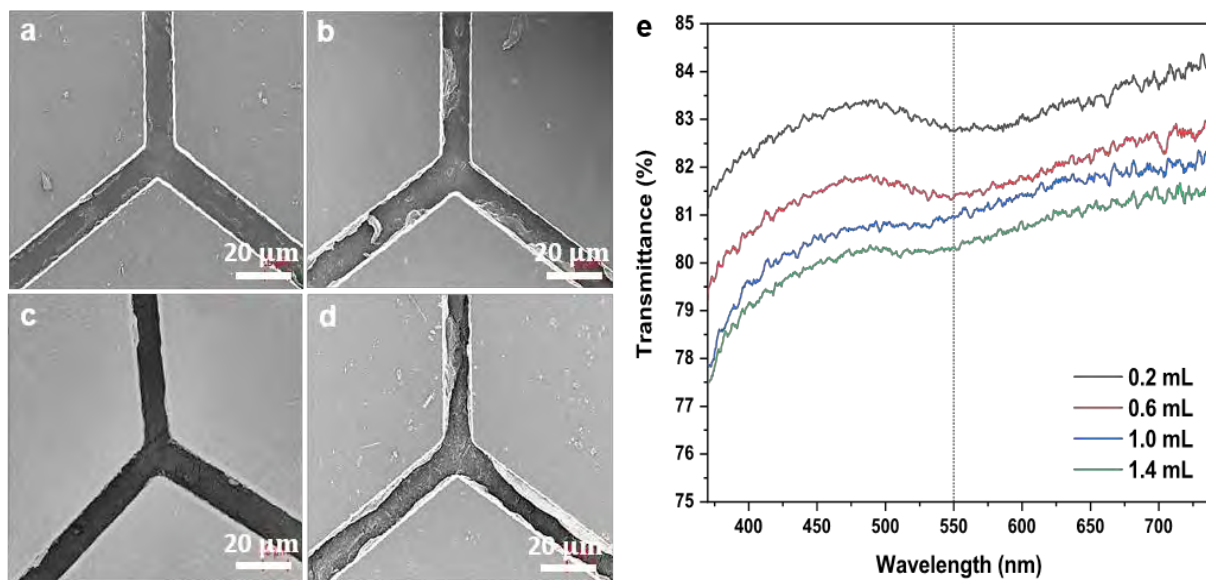


Figure 2. SEM images for different Au NWs spray-coated volumes: 0.2 mL (a), 0.6 mL (b), 1.0 mL (c) and 1.4 mL (d); (e) the transmittances for four Au NWs spray-coated volumes: 0.2 mL, 0.6 mL, 1.0 mL and 1.4 mL.

The total percent transmittance decreases with increasing Au NWs spray-coated volumes. Scanning electron microscope (SEM) images were used to determine the minimum amount of Au NWs that guarantees a uniform coverage of the PDMS channels. The results are shown and compared in **Figures 2a, 2b, 2c** and **2d**. A homogeneous Au NWs layer in the PDMS channels is achieved for a volume of 1 mL. For higher volumes (i.e. 1.4 mL), bulky Au-NWs-compounds have formed on the side walls of the channels; these aggregates are responsible for a major drop in the overall transmittance. At lower volumes, such as 0.2 mL and 0.6 mL, the coverage results incomplete, with several disjointed Au NWs islands on the PDMS substrate. As a successive step, the concentration of MWCNTs of the second layer had to be optimized. Three different concentrations (i.e. 1:6, 1:4 and 1:2 MWCNTs-ethanol) were tested and compared via the total transmittance of the so-obtained devices.

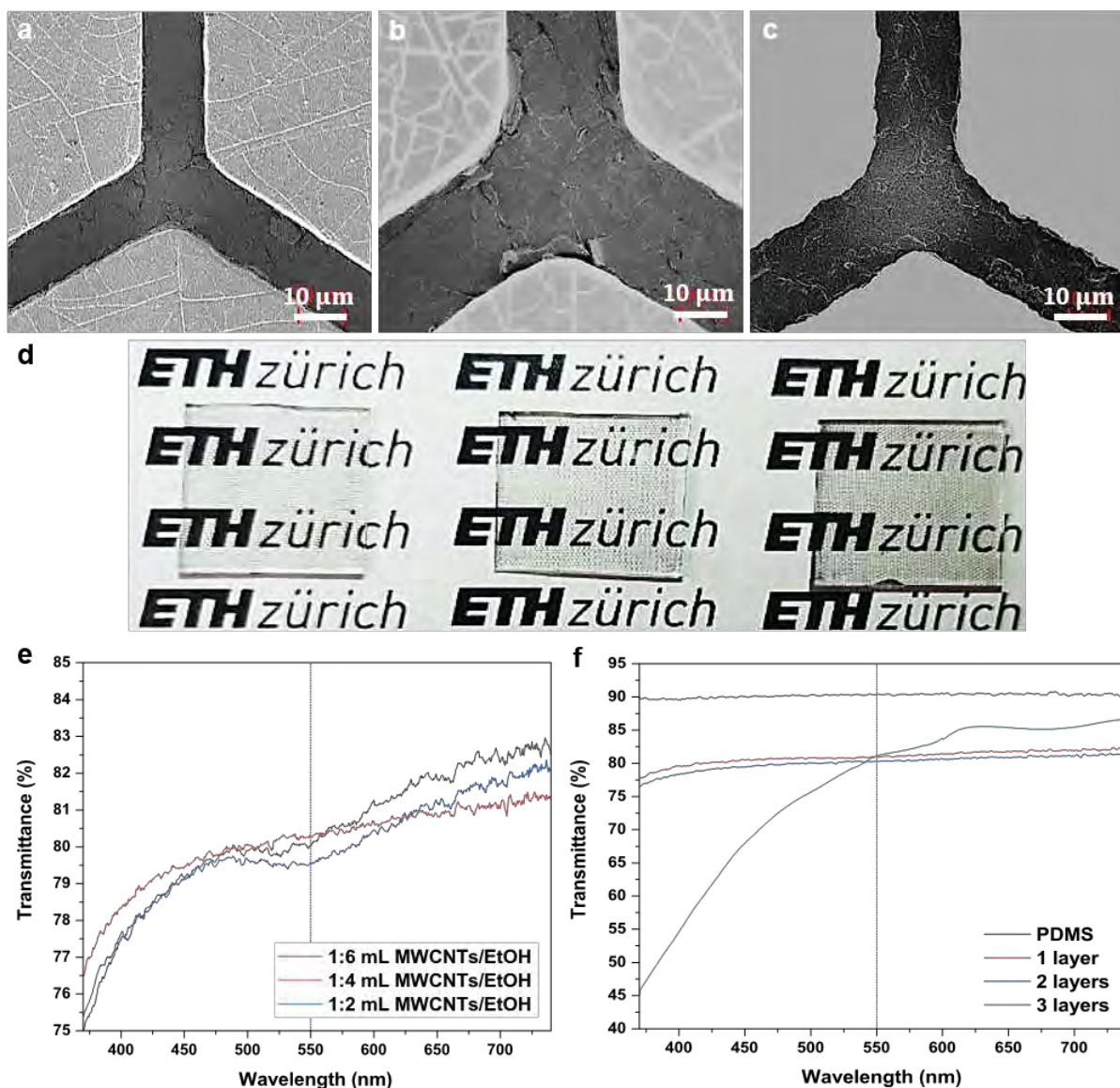


Figure 3. SEM images for different MWCNTs-Ethanol concentrations: 1:6 (a), 1:4 (b) and 1:2 (c); (d) digital pictures for 1-layer (left), 2-layer (middle) and 3-layer (right) current collectors; (e) the transmittances for three MWCNTs-ethanol concentrations: 1:6, 1:4 and 1:2; (f) transmittance in the visible range for current collectors with one, two and three spray-coated layers in the PDMS channels.

Figure 3e displays the total transmittance in the visible range: at a reference wavelength of 550 nm, the transmittances of 80.0%, 80.3% and 79.5% were measured for MWCNTs concentrations of 1:6, 1:4 and 1:2, respectively. **Figures 3a, 3b** and **3c** show the SEM images for each MWCNTs concentration tested. As can be observed, the best coverage was obtained for a MWCNTs concentration in ethanol of 1:4, while for a lower CNT-ethanol ratio (i.e. 1:6) and a higher CNT-ethanol ratio (i.e. 1:2) the channels showed an incomplete coverage and an excess presence of MWCNTs bulky aggregates, respectively. The optimized devices were obtained by spray-coating 1 mL of Au NWs for the first and third layer, and 2 mL of 1:4 ethanol-diluted

MWCNTs for the intermediate layer. **Figure 3d** compares the current collecting nanocomposites with 1 layer, 2 layers and 3 layers of spray-coated materials inside the PDMS channels, respectively. As easily deduced from previous transparency measures, the more the spray-coated layers the less the devices transparency will be. This can be explained by assuming that the more the number of spray-coating stages the PDMS membrane undergoes, the more the number of bulky agglomerates that are formed on the channels side walls; these agglomerates are supposed to be responsible for the major transmittance drop that we observe while increasing the number of layers. A further evidence can be found in **Figure 3f**, where total transmittance in the visible range were collected for the three tested devices. The bare PDMS membrane's transmittance is also shown as a baseline. At a reference wavelength of 550 nm, percent transmittances of 90.4%, 81.0%, 80.3% and 81.1% were measured for a bare PDMS, 1-layer, 2-layer and 3-layer device, respectively. The current collector transmittance effectively decreases with the number of spray-coated layers.

In order to prove the multiscale nanocomposite to be highly stretchable and flexible, we tested it under two main mechanical deformation: stretching and bending. For the stretching tests, the spray-coated PDMS membranes were hooked with two binder clips on two opposite sides; then, they were manually stretched once up to a $\Delta\epsilon\% \approx 100\%$ strain. Digital pictures of the PDMS membranes under stretching are shown in **Figures 4a** and **4b**. As can be seen, the PDMS membranes displayed structural integrity up to 100% strain, without fracturing or breaking phenomena. For the bending tests, the spray-coated PDMS membranes were hooked with two crocodile clips in the middle of two opposite sides; then, they were manually bent once up to an angle of 90° . A picture of the outcome of the bending test on a PDMS membrane is shown in **Figure 4c**. We used a curing agent-elastomer ratio of 1:20; by further increasing the amount of elastomer with respect to the curing agent, the elasticity of the PDMS membrane (and of the entire current collector) will improve. The devices were mounted on a SEM sample holder (**Figure 4h**) and stretched up to different strain levels: $\Delta\epsilon\% = 20\%$, 50% and 100% . As shown in **Figures 4d**, **4e** and **4f**, at a strain of 20% , the microstructure was still intact, without displaying fracturing nor cracking. At a strain of 50% some cracking appeared at the junction points of the PDMS channels; however, the top Au NWs layer still appeared quite homogeneous and compact. Instead, at a strain of 100% , some severe cracking could be observed at the junction points, suggesting a potential increase in overall electrical sheet resistance (see **Figure 4g**).

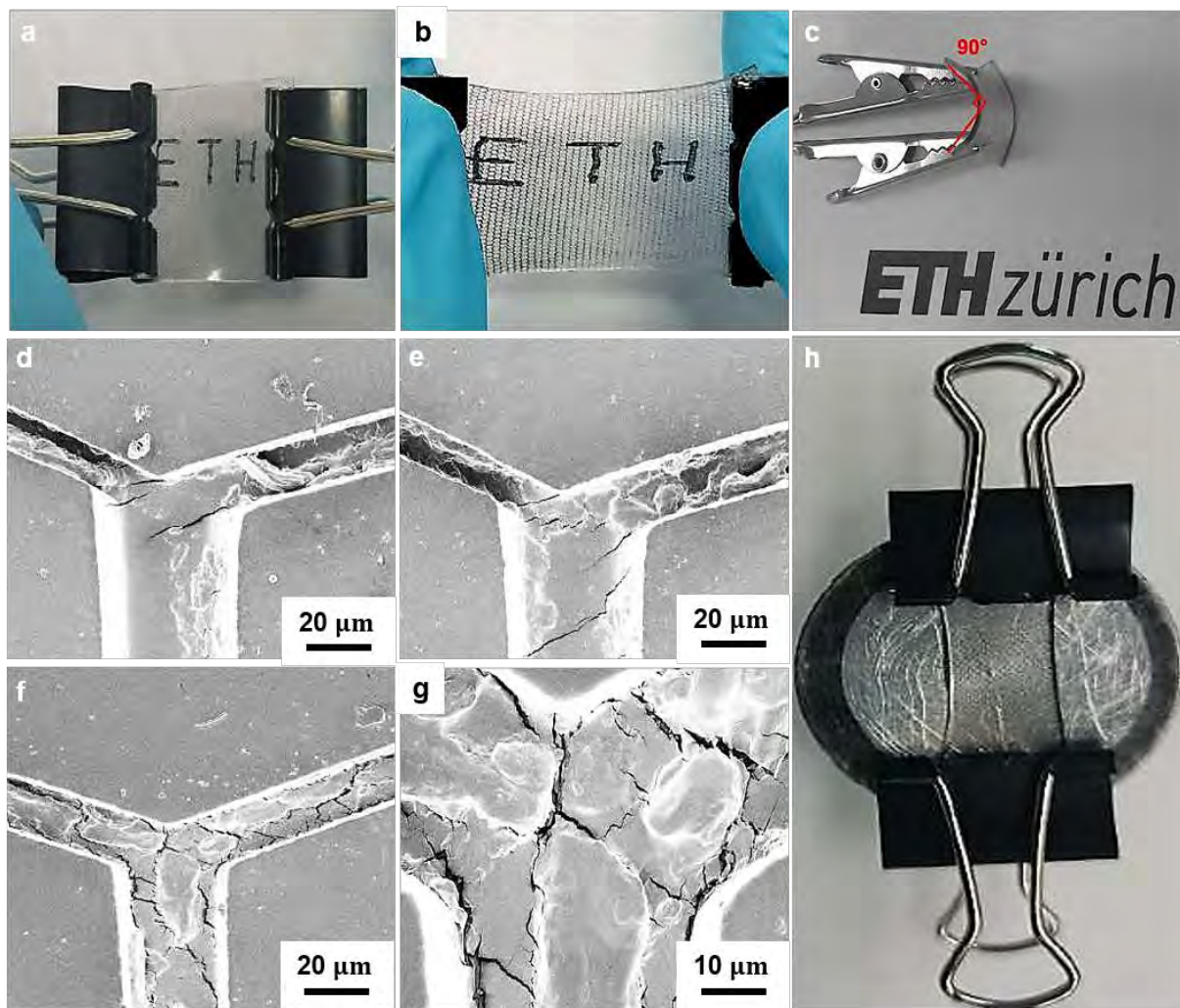


Figure 4. Digital pictures of the PDMS membranes under a $\Delta\varepsilon\% \approx 0\%$ (a) and $\Delta\varepsilon\% \approx 100\%$ (b) stretch; (c) digital picture of the PDMS membrane under $\theta=90^\circ$ bending; SEM images of the current collectors' intra-channel microstructure during uniaxial stretching tests at 20% (d), 50% (e) and 100% (f) strain; (g) magnified detail of the multi-layered structure at the channels' junction points at $\Delta\varepsilon\% \approx 100\%$; (h) sample holder setup for under-stretch SEM imaging.

For the sheet resistance under uniaxial stretching, three identical samples were manually tested for 1000 stretching cycles at three different strain levels: $\Delta\varepsilon\% \approx 20\%$, 50%, 100%. The sheet resistance was measured with a multimeter (Fluke Digital Multimeter 15B+) after each cycle. **Figures 5a, 5b** and **5c** show the experimental setup that was used during each measurement, together with the multimeter displays reporting the no-stretch sheet resistances for each device. The current collectors (2 cm x 2 cm squares with an average thickness of 1 mm) displayed initial sheet resistances of 37.0 ohm/sq, 47.8 ohm/sq and 52.5 ohm/sq. This may suggest a high reproducibility of the hybrid nanocomposites manufacturing process. Quantitative results of the normalized sheet resistances measurements with the number of uniaxial stretching cycles are plotted in **Figure 5f**. We observe an overall increase (up to 25%) in the current collectors sheet

resistance as the number of stretching cycles increases. This result may be due to a progressive loss of contact between the Ag paste (see Experiments section) and the hybrid nanocomposite material in the PDMS channels. In addition, the increasingly severe wrinkling of the multilayered structure may provoke a breaking of the 3-layer structure and the multiscale percolation network, leading to a dramatic increase of the current collector sheet resistance with time and number of deformation cycles. For the sheet resistance under bending, three identical samples were manually tested for 1000 bending cycles at the same fixed bending angle: $\theta=90^\circ$. **Figure 5d** shows the experimental setup that was used during each measurement; a magnified detail of the under-bending membrane is also shown (**Figure 5e**).

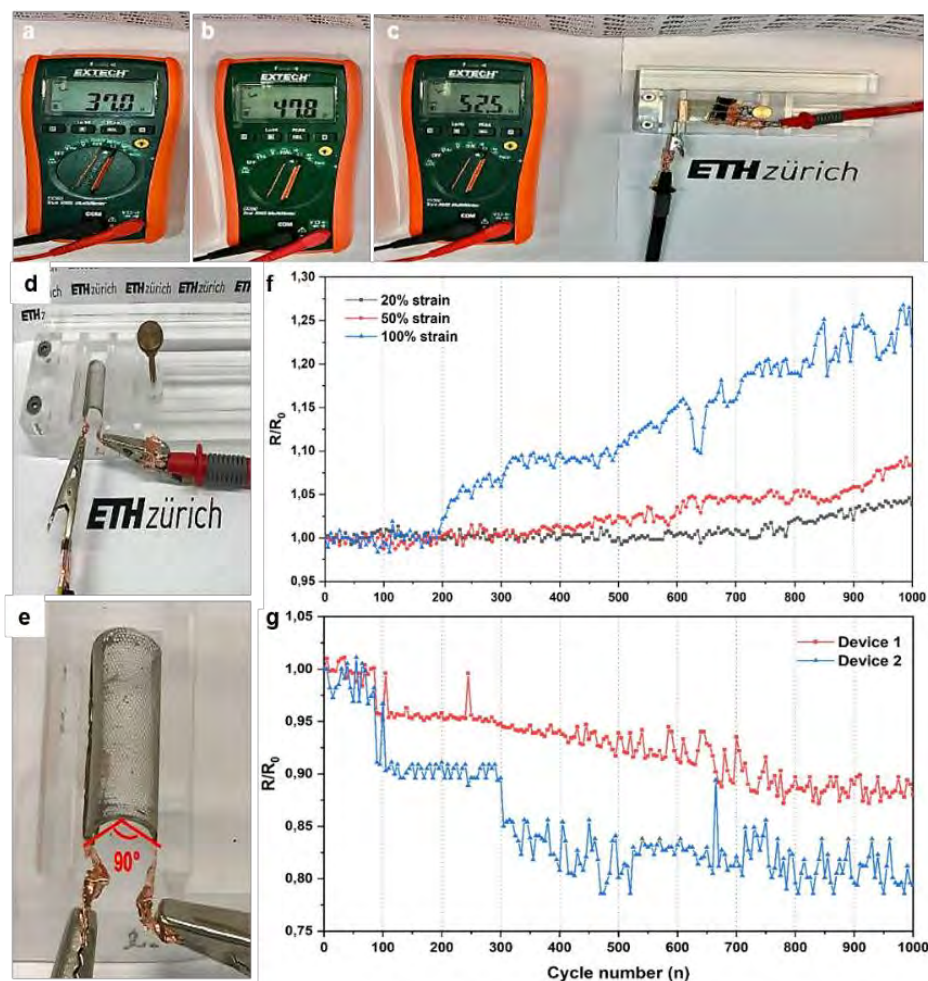


Figure 5. Experimental setup for sheet resistance measurements during 1000 uniaxial stretching cycles (a,b,c) and 1000 bending cycles (d); (e) magnified detail of the under-bending membrane; sheet resistance measurements for each of the 1000 uniaxial stretching cycles (f) and each of the 1000 bending cycles (g).

In **Figure 5g**, an overall decrease (up to 20%) in the sheet resistance is observed as the number of bending cycles increases. During bending, the PDMS membrane leads to normal compression of the Au NWs layer in the channels, as well as inducing an in-plane tension of the Au NWs

percolation network. Secondly, bending could apply a further normal compression on the unwelded Ag NWs junction parts. It is very likely that the previous phenomena generate a slight decrease of the current collector sheet resistance with time and number of applied bending cycles.

Conclusion

We manufactured and optimized a hierarchical multiscale hybrid nanocomposite current collector for applications in Li-ion batteries. Highly stretchable, transparent and conductive devices films were realized by combining the enhanced mechanical compliance and optical transparency of small MWCNTs ($\varnothing \approx 11$ nm, $L \approx 5-20$ μm) and the enhanced electrical conductivity of relatively longer Au NWs ($\varnothing \approx 3$ nm, $L \approx 50-100$ μm) backbone. The structure can provide efficient multiscale electron transport paths with Au NWs as a main current backbone collector and MWCNTs a local elastic percolation network. Indeed, our devices showed much superior and robust mechanical compliance, electrical conductivity and optical transmittance over single component materials such as Au NWs only or MWCNTs only conductors. The Au NWs/MWCNTs/Au NWs hybrid current collector demonstrated to be

- conductive (average resistance of 40-50 ohms);
- transparent (T: 80-85%);
- highly stretchable (up to 100% strain);
- with remarkable mechanical reliability over long repeated bending-stretching cycles (1000 cycles).

Experiments

Synthesis of Au NWs: Gold nanowires (Au NWs) were utilized due to gold high electrical conductivity ($EC \approx 4.52 \cdot 10^5$ S/cm)¹³. Au nanowires are synthesized by successive multistep growth^{17,18}. This method allows the production of high quality ultrathin Au NWs with uniform

diameter of approximately 3 nm and length up to $\approx 4 \mu\text{m}$. The actual procedure involves 4 chemicals (HAuCl_4 , oleylamine, n-hexane and Triisopropylsilane (TIPS)) which were used throughout the entire synthetic process: n-hexane served as solvent, oleylamine as surface capping agent and TIPS as reducing agent. The Au NWs are synthesized at room temperature.

In a glove box, 0.1 g of $\text{HAuCl}_4 \cdot 3\text{H}_2\text{O}$ powder (99.99%, abcr GmbH) and 15.35 mL of n hexane (95%, Sigma-Aldrich) were mixed and stirred for 5 min. After that, 4.55 mL of oleylamine ($\geq 70\%$, technical grade from Sigma-Aldrich) were added, followed by a 5 min stirring. At this stage of the process, the resulting solution was transparent yellowish red. 6.55 mL of Triisopropylsilane (TIPS) were finally added to the solution, again followed by stirring for 5 min. The final resulting yellowish solution was aged at room temperature ($20\text{-}25^\circ\text{C}$) for 12 hours. During this aging process, purple suspension was formed. Separation of the Au NWs requires thorough washing with mixed solvents (1:4): 20 ml of ethanol and 5 mL of methanol. After that, the supernatant was removed and the remaining precipitate was re-dispersed in 12.6 mL of cyclohexane ($\geq 99.5\%$ purity, Sigma-Aldrich). The finally cyclohexane-dispersed Au-NWs were stored at 5°C with nitrogen gas (N_2). A simplified scheme of the overall synthesis procedure for the Au NWs is shown in **Figure S1a**.

MWCNTs preparation: High purity COOH-functionalized graphitized MWCNTs with an external diameter of approximately 30 nm (purity of 99%wt, Iljin Nanotech) produced by an arc-discharge method were dispersed in an ethanol solution, sonicated, and then centrifuged. A concentration of 4 mg/mL was chosen as the initial MWCNTs-COOH/ethanol concentration. **Figures S1b** and **S1c** show the Au NWs and MWCNTs suspensions obtained just after dispersion in cyclohexane and ethanol, respectively. These well dispersed suspensions make the batch suitable for many deposition techniques, such as spray-coating.

Current collector preparation: We fabricated stretchable transparent electrodes with regularly patterned channels carved in an elastomeric substrate, poly-dimethylsiloxane (PDMS). The fabrication process for the textured PDMS membrane includes two major steps: photolithography, and elastomer casting and curing. The hexagonal grid photoresist on silicon wafer was fabricated in cleanroom. In the second step, after cleaning the grid with ethanol, a layer of PDMS prepolymer (Sylgard 184 kit, 20:1 mixed ratio) is cast on the silicon wafer, and cured after degassing in an oven at 60°C for 20 min. The cured PDMS substrate is then peeled off from the silicon wafer with the hexagonal channel carved on one side. Finally, the cured PDMS substrate is cut with a blade into 2 cm x 2 cm squares.

In order to realize the multilayered structure inside the PDMS channels, spray-coating technique was exploited. After attaching each PDMS membrane to a Petri dish, a certain volume of Au NWs was spray-coated with a spray gun on the membranes at a pressure of circa 0.5 bar at room temperature. Subsequently, the devices were O₂ plasma-treated for 30 min in order to make the Au NWs carpet (first layer) in the channels hydrophilic. Hydrophilicity of each Au NWs layer is fundamental to guarantee the maximum adhesion with the intermediate layer of COOH-functionalized MWCNTs. After plasma treatment, the spray-coating process was repeated on a hot plate at 40°C with MWCNTs at a certain concentration: the second layer (i.e. intermediate carbon nanotubes carpet) is now realized. Spray-coating was iterated one last time at room temperature using Au NWs; in this way, all three layers have been deposited in the PDMS channels. Finally, the complete device underwent the O₂ plasma process again, so that the third Au NWs layer conductivity could be increased. It is important to underline that after each spray-coating stage, the membranes were cleaned multiple times using different adhesive tapes. The spray-coating equipment and the Petri-dish-membrane setup are shown in **Figure S2d**.

Stability of the electrical conductivity under stretching and bending is a critical issue for stretchable electrode. In order to measure the sheet resistance of the current collectors, it is necessary to ensure reliable contact between the electrodes and the multimeter probes. Liquid Ag ink was deposited on the contact regions; then, each device was heated for 20 min at 140°C in an oven to make the Ag ink dry. This entire process was repeated 5 times per device in order to achieve the maximum contact between the multi-layered structure inside the PDMS channels and the Ag ink. Secondly, ethanol-diluted Ag paste was applied once on the contact regions, followed by a 45 min drying process at 140°C in an oven. Finally, conductive copper tape was attached on the dried Ag paste on both sides of the PDMS membrane.

Material characterization: The morphologies of the synthesized Au NWs and the MWCNTs were analyzed by transmission electron microscopy (TEM, Hitachi HT 7700 EXALENS at an accelerating voltage of 100 kV and JEOL JEM-1400 Plus at an accelerating voltage of 150 kV) at low and high magnification (see **Figures S1d, S1e and S1f**). The morphology of electrodes was studied by scanning electron microscopy (SEM) on a LEO 1530 Gemini.

Optimization of the spray-coating pressure: We tested 2 different nitrogen pressures for the MWCNT-carpet deposition and compared the different results using a scanning electron microscope (SEM). As can be seen in **Figures S2b**, the best result in terms of deposition homogeneity was achieved for the lowest nitrogen pressure (i.e. 0.5 bar); this is also confirmed

in the SEM image of **Figure S2c** where a dense, compact and relatively homogeneous MWCNTs carpet was achieved. A higher pressure (i.e. 1.5 bar) leads to an incomplete coverage of the PDMS channels (**Figure S2a**).

EDX mapping analysis: EDX mapping of a 3-layer hybrid current collector can be found in **Figure S2e**. We have the confirmation that the material inside the channels is predominantly gold; in this case, the gold EDX signal (in yellow) corresponds to the third spray-coated layer of Au NWs. In addition, we can further verify that the flexible transparent membrane is effectively made of polydimethylsiloxane (PDMS): in the regions around the channels, the EDX mapping shows a percent elemental composition of carbon, oxygen and silicon which is coherent with the expected polydimethylsiloxane.

References

1. J. Kim, M. Lee, H. J. Shim, R. Ghaari, H. R. Cho, D. Son, Y. H. Jung, M. Soh, C. Choi, S. Jung, et al., *Nature communications* **2014**.
2. W. Zeng, L. Shu, Q. Li, S. Chen, F. Wang, X.-M. Tao, *Advanced materials* **2014**, *26*, 5310-5336.
3. S. Ye, A. R. Rathmell, Z. Chen, I. E. Stewart, B. J. Wiley, *Advanced materials* **2014**, *26*, 6670-6687.
4. E. Artukovic, M. Kaempgen, D. Hecht, S. Roth, G. Gurner, *Nano letters* **2005**, *5*, 757-760.
5. M. Zhang, S. Fang, A. A. Zakhidov, S. B. Lee, A. E. Aliev, C. D. Williams, K. R. Atkinson, R. H. Baughman, *Science* **2005**, 309.
6. S. Bae, H. Kim, Y. Lee, X. Xu, J.-S. Park, Y. Zheng, J. Balakrishnan, T. Lei, H. R. Kim, Y. I. Song, et al., *Nature nanotechnology* **2010**, *5*, 574.
7. G. Eda, G. Fanchini, M. Chhowalla, *Nature nanotechnology* **2008**, *3*, 270-274.
8. J. Lee, P. Lee, H. Lee, D. Lee, S. S. Lee, S. H. Ko, *Nanoscale* **2012**, *4*, 6408-6414.
9. S. De, T. M. Higgins, P. E. Lyons, E. M. Doherty, P. N. Nirmalraj, W. J. Blau, J. J. Boland, J. N. Coleman, *ACS nano* **2009**, *3*, 1767-1774.
10. J.-Y. Lee, S. T. Connor, Y. Cui, P. Peumans, *Nano letters* **2008**, *8*.
11. P. Lee, J. Ham, J. Lee, S. Hong, S. Han, Y. D. Suh, S. E. Lee, J. Yeo, S. S. Lee, D. Lee, et al., *Advanced Functional Materials* **2014**, *24*, 5618.
12. Yun, Y. S. et al., *Synthetic Materials* **2012**, *162*, 1364-1368.
13. H. Feng, Y. Yang, Y. You, G. Li, J. Guo, T. Yu, Z. Shen, T. Wu, B. Xing, *Chemical Communications* **2009**, 1984-1986.
14. Azadmanjiri, Jalal et al., *RSC advances* **2016**, *109*, 361-385.
15. Zhang, Shuai et al., *Nano letters* **2018**, 6030-6036.
16. R. A. Serway, Fort Worth, Texas; London: *Saunders College Pub*, tech. rep., **1998**.
17. Z. Huo, C.-k. Tsung, W. Huang, X. Zhang, P. Yang, *Nano letters* **2008**, *8*, 2041-2044.
18. A. Khan, S. Lee, T. Jang, Z. Xiong, C. Zhang, J. Tang, L. J. Guo, *Small* **2016**, *12*, 3021-3030.

Supporting information

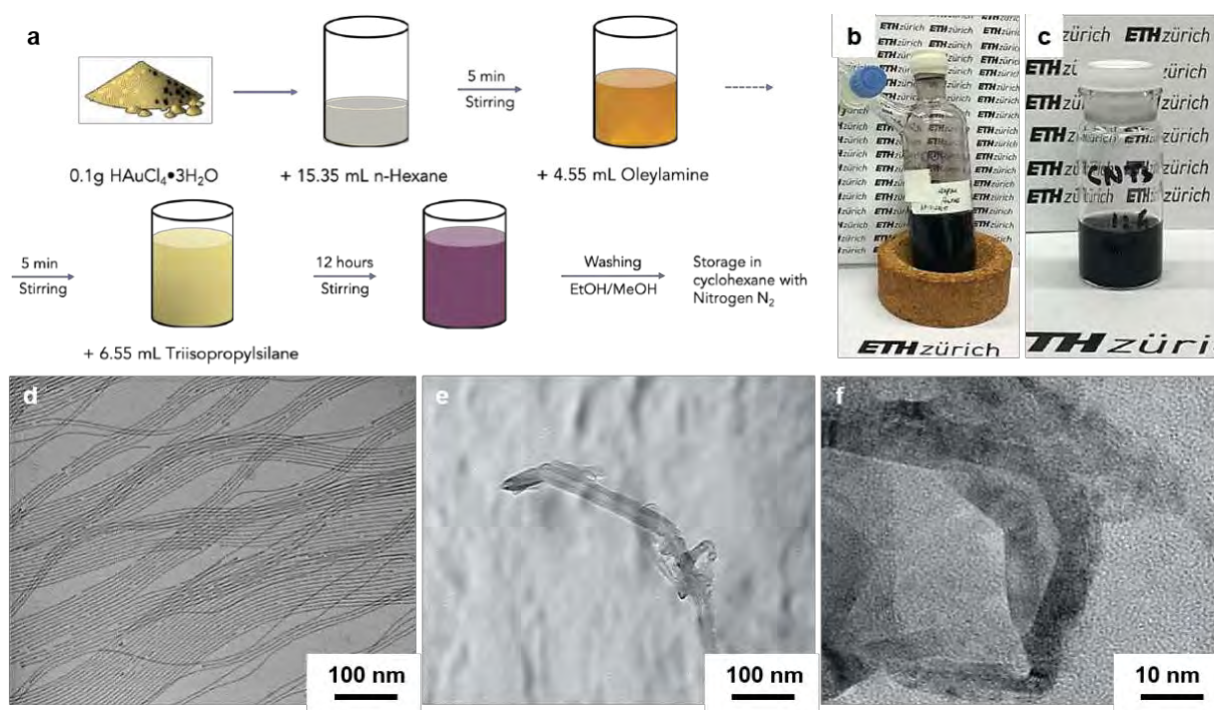


Figure S1. (a) Simplified scheme of the overall synthesis procedure for the Au NWs; (b) Au NWs-cyclohexane suspension; (c) MWCNTs-ethanol suspension; TEM pictures of Au NWs (d) and MWCNTs (e,f).

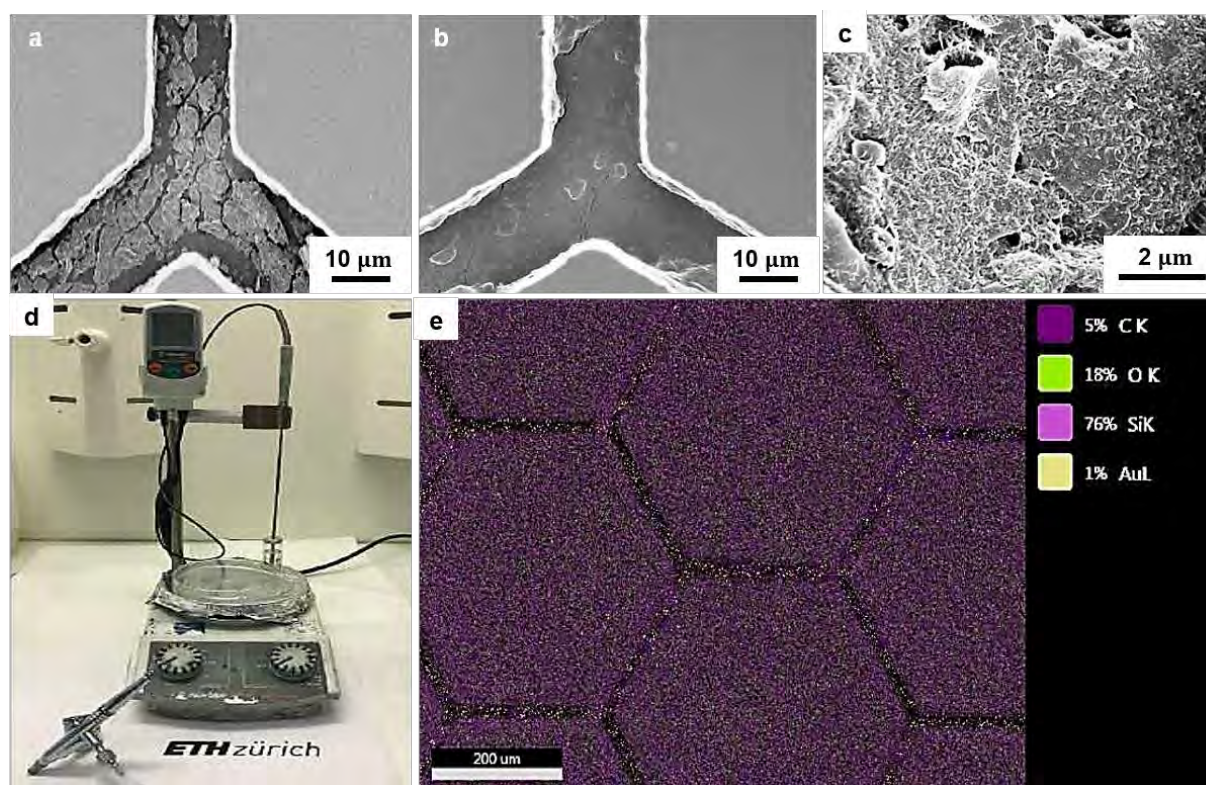


Figure S2. SEM pictures of MWCNT carpets inside the PDMS channels, spray-coated at a nitrogen pressure of 1.5 bar (a) and 0.5 bar (b); (c) magnified SEM detail of the MWCNT carpet obtained at a pressure of 0.5 bar; (d) spray-coating equipment setup; (e) EDX mapping of Au NWs/MWCNTs/Au NWs current collector.